Reports

Near-Earth Asteroids: Possible Sources from Reflectance Spectroscopy

Abstract. *Spectra of near-Earth asteroids were compared to spectra of selected asteroids, planets, and satellites to determine possible source regions. The diversity of reflectance spectra of the near-Earth asteroids implies different mineralogical compositions and hence more than one source region. The presence of near-Earth asteroid spectral signatures similar to those of certain main-belt asteroids supports models that derive some of these asteroids from the 5:2 Kirkwood gap and the Flora family by gravitational perturbations. Planetary and satellite surfaces are different in composition than the near-Earth asteroids, which is in agreement with theoretical arguments that such bodies should not be sources. Some near-Earth asteroids supply portions of Earth's meteorite flux, but other sources must also contribute.*

LUCY A. MCFADDEN
Astronomy Program, University of Maryland, College Park 20742
MICHAEL J. GAFFEY*
THOMAS B. MCCORD
Planetary Geosciences Division, Hawaii Institute of Geophysics, University of Hawaii, Honolulu 96822

*Present address: Department of Geology, Rensselaer Polytechnic Institute, Troy, N.Y. 12181.

Among solar system objects are a group of small asteroids that temporarily (mean lifetime, $\sim 10^7$ to 10^9 years) occupy orbits crossing those of some or all of the terrestrial planets. These asteroids have not been explored by spacecraft and have only recently been studied remotely from ground-based telescopes. They include the Apollos, with orbits crossing that of Earth; the Atens, a subset of Apollos with semimajor axes less than that of Earth's orbit; and Amors, with orbits that cross that of Mars and approach Earth. These bodies, collectively called near-Earth asteroids (NEA's), are defined as solid bodies that are large enough to be seen with a telescope and have a perihelion distance less than that of Mars.

Clues to the evolution of small bodies in the solar system can be derived from knowledge of their places of origin. Unlike the asteroids of the main belt between Mars and Jupiter, the orbits of NEA's are not stable over the lifetime of the solar system (*1*). They collide with planets or are ejected from the solar system, thus requiring a source and mechanism that places them in planet-crossing orbits. Hypothesized source regions include asteroids near dynamically unstable regions of the main belt (Kirkwood gaps and secular resonances) (*2, 3*) and volatile-free remnants of comets (*4*). Understanding the relation of NEA's to meteorites should help constrain mechanisms resulting in collisions with the earth (*5*). There are currently 83 known NEA's. Their possible source regions and the relations of NEA's to meteorites are examined through mineralogical interpretation of 17 NEA reflectance spectra (*6, 7*).

Determining genetic links or relations between NEA's and other solar system objects is hindered by the absence of field relations (the object is not found with its parent body). Since mineralogy is controlled by initial chemistry, temperature, and pressure, the presence of the same minerals in the same proportions on two different solar system objects implies that they underwent a similar evolution and may have formed in the same region of the solar system. In this analysis, two objects are inferred to have the same minerals present in the same proportions if their reflectance spectra and albedo agree to within experimental error (Fig. 1). This technique is convincing when absorption bands that are diagnostic of particular minerals are present. Spectral reflectance measurements of mineral mixtures, controlled for composition and relative abundance, have been studied in the laboratory to relate these variables to absorption band characteristics (band position, strength, and width). The albedo criterion may account for the presence or absence of a spectrally neutral absorber (such as elemental carbon or certain spinels). Particle size, possibly controlled by primary processes such as cooling rate or secondary regolith-forming processes (collisions), is also expected to affect the albedo. The strength of an absorption band is a function of particle size. It is possible that the two criteria for determining mineralogical similarity eliminate truly related objects if one underwent either preferential comminution of its mineral constituents or lost a fine-grained regolith, leaving a bare rock of larger grains. We assume that the optical properties of asteroid surfaces have not been significantly altered by secondary processes since there is generally no observational evidence for this (*8*). Another interpretive constraint is that not all asteroid spectra have prominent absorption bands. In this case there is uncertainty in the interpretive technique that cannot be evaluated, but the presence of strongly featured minerals can be ruled out.

We evaluated the NEA spectra (*6, 7*) and previously measured spectra of about 300 asteroids (*9*) and of other planetary surfaces (*10*). These data are not uniform in terms of spectral coverage and signal-to-noise ratio. If no albedo measurement exists or there is limited overlap of spectral coverage, a mineralogical and petrological similarity is only suggested. We compared reflectance and

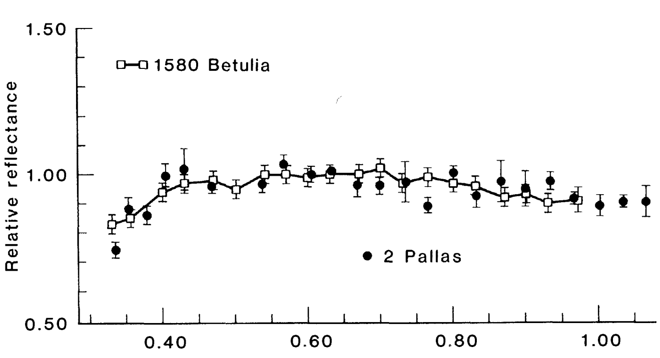

Fig. 1. Reflectance spectra of two asteroids that agree to within experimental error. Albedo of 1580 Betulia is 0.03 to 0.06, albedo of Pallas is 0.06, from radiometric measurements. Spectra are scaled to 1.0 at 0.56 μm by convention.

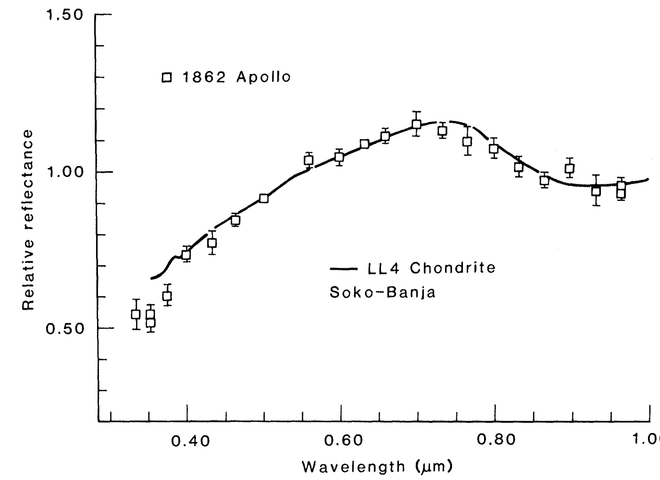

Fig. 2. Scaled (to 1.0 at 0.56 μm) reflectance spectrum of an NEA and a meteorite powder that agree to within experimental error.

albedo of NEA's with those of planets and satellites in the solar system. Because we assumed that the composition of asteroids which have been perturbed from resonances and Kirkwood gaps in the main belt is similar to those now near these regions, we examined genetic links by comparing their reflectance and albedo with those of NEA's.

Meteoritic assemblages have been classified on the basis of spectral features and albedo (*11*). Comparison of spectra of meteorites and NEA's (Fig. 2) were made under the assumption that the texture of the asteroids is similar to powdered meteorite samples. Previously measured meteorites are from interior portions of selected specimens for which the effects of terrestrial weathering, which results in a distinctive spectral signature, are negligible. The relation between mineralogy and reflectance spectra of meteorites has been established by direct measurements. Differences in reflectance larger than experimental error indicate the presence of different minerals, different proportions of the same minerals, or different textures.

None of the NEA's showed the spectral characteristics of known geological units on the moon, Mercury, Mars, or the satellites of the outer solar system. Most had strong ultraviolet and near infrared absorption bands, indicating the presence of mafic silicates (most commonly olivine and pyroxene) and the absence of materials and physical processes that would mask these absorptions (*6, 7*). Only 40 percent of the main-belt asteroids have these features, whereas 75 percent of NEA's have them.

Reflectance spectra for 32 main-belt asteroids within 0.1 AU of the 5:2 Kirkwood gap were compared with NEA spectra. Four NEA's showed reflectance spectra and albedos similar to seven main-belt asteroids near the 5:2 Kirkwood gap (Table 1) (*12*). The spectra indicated a plausible genetic relation between 1580 Betulia, an Amor-type NEA, and 2 Pallas, a large main-belt asteroid with a distinct reflectance spectrum (Fig. 1). The orbit of 2 Pallas is close to the 5:2 Kirkwood gap. Spectral analysis of 1685 Toro (an Apollo-type NEA) suggests mineralogical similarity to asteroid 349 Dembowska, also located near the 5:2 Kirkwood gap (*7*). The NEA's 1036 Ganymed (*13*) and 1620 Geographos, whose spectra are indistinguishable, have the same reflectance and albedo as five other asteroids near the 5:2 Kirkwood gap (Table 1).

Near the ν_6 resonance, there is one suggested analog, 18 Melpomene, to an NEA. There are 11 previously measured spectra (*9*) in or near the ν_6 resonance (*14*). Among 18 members of the Flora family, which is also located near the ν_6 resonance, 1036 Ganymed and 1620 Geographos have similar spectral reflectance and albedo as 1058 Grubba (*15*). In addition, there are three suggested analogs to seven other members of the Flora family (Table 1).

The NEA 1915 Quetzalcoatl has a mineralogical composition similar to one hemisphere of the main-belt asteroid 4 Vesta (Fig. 3). Vesta is located in a stable region of the asteroid belt. This is so far the only analog found to an NEA that is not associated with a dynamical family or gravitationally depleted region of the asteroid belt.

Among the 73 main-belt asteroids crossing Mars' orbit (excluding the Amors), seven have measured reflectance spectra (*16*). None of these were found to be spectrally similar to the measured population of NEA's. Only three members of the Phocaea family (*17*) have measured reflectance spectra; none show mineralogic similarity to any measured NEA. The 3:1 Kirkwood gap region, proposed as a major source of ordinary chondrites (*2*), is poorly sampled. Among 7 of 14 asteroids near the 2:1 Kirkwood gap (*18*), none had spectral features similar to those of NEA's.

Table 1. Near-Earth asteroids and plausible main-belt parent bodies.

Near-Earth asteroides	Main-belt asteroids
	5:2 Kirkwood gap
1580 Betulia	2 Pallas
1685 Toro	349 Dembowska
1036 Ganymed, 1620 Geographos	68 Leto
1036 Ganymed, 1620 Geographos	471 Papagena
1036 Ganymed, 1620 Geographos	354 Eleonora
1036 Ganymed, 1620 Geographos	39 Laetitia
1036 Ganymed, 1620 Geographos	532 Herculina
	ν_6
3102 1981QA	18 Melpomene
	Flora family
1620 Geographos, 1036 Ganymed	1058 Grubba
887 Alinda, 1036 Ganymed	1055 Tynka
887 Alinda, 3102 1981QA	1830 Pogson
1036 Ganymed	453 Tea
1862 Apollo	1088 Mitaka
3102 1981QA	1449 Virtanen
3102 1981QA	341 California

Meteoritic analogs of type 3 carbonaceous chondrites (C3), LL4 ordinary chondrites (Fig. 2), and the diogenite subclass of basaltic achondrites were found from comparisons with NEA reflectance spectra. With an albedo measurement the interpretation of the spectrum of 1980AA may result in the finding of an additional ordinary chondrite analog to black, shocked chondrites (the albedo must be low). An albedo measurement should also discriminate between two possible interpretations of NEA 3102 1981QA, which may be a C3 or type 6 enstatite chondrite (E6) as judged by its reflectance spectrum. The spectrum of the Aten asteroid 2100 Ra-Shalom, was not characteristic of either a type 2 (C2) or C3. It was interpreted to be a more olivine-rich C2 assemblage or intermediate between C2 and C3.

No meteoritic analogs were found for five NEA spectra (*19*). This suggests the presence of asteroidal assemblages that are not represented in the meteorite collection. In addition, irons and many types of chondrites and basaltic achondrites are not represented.

The absence of NEA's similar in composition to the satellites of the outer solar system is consistent with the theory of the chemical composition of the outer solar system (*20*) that predicts the presence of low-temperature conden-

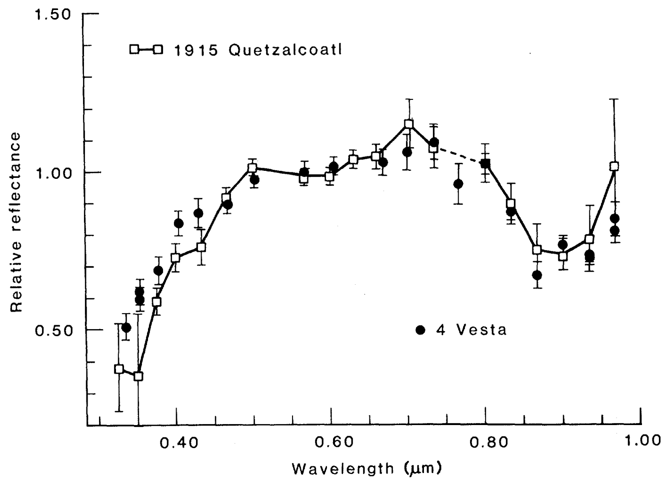

Fig. 3. Orthopyroxene dominated hemisphere of 4 Vesta compared to 1915 Quetzalcoatl, two basaltic achondrite analogs in the solar system. Datum at 0.76 μm of the NEA is deleted as a result of nonlinear atmospheric fluctuations in O_2.

sates from the solar nebula at large heliocentric distances. These assemblages are apparently not common in the near-Earth population.

Differences in spectral reflectance greater than the experimental error among the NEA's (*6, 7*) imply different surface compositions and multiple parent bodies or origin from different regions of a large parent body. These parent bodies appear to be in different dynamical regions of the asteroid belt, although some candidates are found in more than one source region.

The compositional structure of the main asteroid belt has been described in three different data sets (*21*). In the inner asteroid belt, the predominance of high-albedo asteroids which are highly reflective in the near infrared and have strong ultraviolet absorptions and near infrared absorption bands of varying strength (taxonomic type S), is well established. Some NEA's have surface compositions similar to these asteroids. It is therefore likely that 1036 Ganymed, 1620 Geographos, and 433 Eros originated from the inner belt. Dynamical considerations are consistent with this experimentally derived correlation for some regions of the inner belt such as the 5:2 Kirkwood gap and possibly the Flora family.

Both 1580 Betulia and 2 Pallas have high orbital inclinations (52° and 35°, respectively) in addition to inferred similar surface composition. That only two of all measured asteroids have this spectrum and albedo further supports a possible genetic link between these two objects. These observational results indicate a plausible dynamical relation between them.

Observational evidence indicates that 1915 Quetzalcoatl has a surface assemblage similar to one hemisphere of 4 Vesta. Although Vesta is the only known main-belt asteroid with a basaltic achondrite-type assemblage, dynamics apparently argue against Vesta being the actual parent body of this meteorite class (*22*). The presence of such an assemblage on a NEA provides a more dynamically favored parent for these meteorites. But the presence of only two known basaltic achondrite parent body candidates, one in a short-lived orbit, does not eliminate a possible relation between Vesta and Quetzalcoatl. The absence or rarity of analogs among Mars-crossers, the Phocaea family, and the ν_6 resonance cannot be considered significant without a wider sample of these asteroids.

The absence of analogs to NEA's near the 2:1 resonance will probably hold true since spectra of 50 percent of the population with diameters greater than 60 km have been examined. The predominance of S type NEA's compared to the dark (taxonomic type C) spectrally neutral asteroids common near the 2:1 Kirkwood gap support this conclusion (*21*). Observational data do not support the 2:1 Kirkwood gap as a source region of NEA's.

The C3 meteoritic analog (887 Alinda) has a strong ultraviolet and weak 1.0-μm absorption. It would be classified according to asteroid taxonomy as an S type but is not to be confused with the low-albedo, spectrally flat C-type asteroids.

The LL4 ordinary chondrite analog 1862 Apollo more closely matches the spectral features and albedo of LL4-type spectra than asteroids previously designated as ordinary chondrite analogs (*23*). New data argue against these previous designations (*7*). And 1862 Apollo has broadband photometric properties that are statistically different from those of S-type asteroids and from previously designated ordinary chondrite analogs (*24*). Apparently, few if any S-type asteroids are ordinary chondrite analogs (*25*). The conditions for the delivery and survival of meteorites (*26*) are sufficiently stringent to preclude the assumption that all asteroid compositions are represented in the meteorite collection.

The absence of analogs to the diverse group of metallic iron meteorites supports models concluding that their sources are in orbits with longer mean lifetimes than the NEA's (*5*). The asteroids for which no meteoritic analogs were found apparently do not contribute significantly to the meteorite population or else have not yet been recovered as meteorites. The parent bodies of meteorites for which there are presently no analogs among NEA's may simply be (i) as yet undiscovered or characterized, (ii) too small to be studied as asteroids or (iii) located in regions where asteroids have not yet been found, such as the Lagrangian points of the earth-sun system (*27*).

References and Notes

1. E. J. Öpik, *Proc. R. Irish Acad.* **54A**, 165 (1951); J. R. Arnold, in *Isotopic and Cosmic Chemistry*, H. Craig, S. L. Miller, G. J. Wasserberg, Eds. (North-Holland, Amsterdam, 1964), p. 347.
2. G. W. Wetherill, *Meteoritics* **10**, 1 (1985).
3. P. D. Zimmerman and G. W. Wetherill, *Science* **182**, 51 (1973); H. Scholl and C. Froeschlé in *Comets, Asteroids, Meteorites—Interrelations, Evolution and Origins*, A. H. Delsemme, Ed. (Univ. of Toledo Press, Toledo, 1977), pp. 293–295; J. G. Williams and J. Faulkner, *Icarus* **46**, 390 (1981).
4. G. W. Wetherill, *Icarus* **37**, 96 (1979); E. J. Öpik, *Adv. Astron. Astrophys.* **2**, 219 (1963).
5. G. W. Wetherill and J. G. Williams, *J. Geophys. Res.* **73**, 635 (1968); G. W. Wetherill, *Geochim. Cosmochim. Acta.* **40**, 1297 (1976); R. Greenberg and C. R. Chapman, *Icarus* **55**, 455 (1983).
6. L. A. McFadden, M. J. Gaffey, T. B. McCord, *Icarus* **58**, 25 (1984).
7. L. A. McFadden, thesis, University of Hawaii, Honolulu (1983).
8. D. L. Matson *et al.*, in *Proc. Lunar Sci. Conf. 7* (1976), p. 3603; however, King *et al.* [*Lunar Planet. Conf. 15* (1984), p. 429] suggest that a few measured asteroid spectra may show evidence of lunar-like secondary alteration.
9. C. R. Chapman and M. J. Gaffey, in *Asteroids*, T. Gehrels, Ed. (Univ. of Arizona Press, Tucson, 1979), pp. 655–687.
10. T. B. McCord and D. P. Cruikshank, in *Infrared Astronomy* (Proceedings of the IAU Symposium 96), G. C. Wynn-Williams and D. P. Cruikshank, Eds. (Kluwer Boston, Hingham, Mass., 1981), pp. 57–87.
11. M. J. Gaffey, *J. Geophys. Res.* **81**, 905 (1976).
12. Asteroids near the 5:2 Kirkwood gap with measured reflectance spectra not like spectra of any of the NEA's measured to date include 1, 16, 22, 28, 41, 45, 71, 88, 110, 128, 129, 139, 140, 156, 185, 200, 216, 236, 308, 356, 386, 441, 446, and 674. These asteroids are ruled out as possible parent bodies for the NEA's.
13. J. Gradie and E. Tedesco, unpublished albedo.
14. Asteroids in the ν_6 resonance [J. G. Williams, in *Asteroids*, T. Gehrels, Ed. (Univ. of Arizona Press, Tucson, 1979), pp. 1040–1063] with measured reflectance spectra include 36, 130, 413, 426, 739, and 1317. In addition, asteroids 6, 18, 80, 313, and 344 are large asteroids sufficiently near the resonance to be parent body candidates. All of these except 18 Melpomene can be excluded as possible parent bodies of any NEA measured to date.
15. Members of the Flora family [Y. Kozai, in *Asteroids*, T. Gehrels, Ed. (Univ. of Arizona Press, Tucson, 1979), pp. 334–358] with measured reflectance spectra that can be excluded as possible NEA parent bodies include 8, 40, 43, 149, 281, 341, 574, 770, 782, 1636, and 1717.
16. Mars-crossers with perihelion ≤ 1.66 AU (excluding the NEA's) with measured reflectance spectra include 313, 391, 574, 1088, 1656, 1717, and 1727.

17. Phocaea family asteroids with measured reflectance spectra are: 25, 323, 326.
18. Asteroids greater than 60 km in diameter within 0.1 AU of the 2:1 Kirkwood gap with measured reflectance spectra include 92, 106, 108, 122, 175, 511, and 895.
19. NEA's 1580, 1685, 1943, 2201, and 1979VA have no meteoritic analogs; 1627 Ivar does not either, but its spectrum is too noisy to be useful; 433 is a stony-iron analog as judged by infrared spectra not addressed in this work; 1036 and 1620 have no meteoritic analogs, but spectral coverage is not sufficient to conclude that they are different in composition than any meteoritic type.
20. J. S. Lewis, *Space Sci. Rev.* **14**, 401 (1973).
21. J. Gradie and E. Tedesco, *Science* **216**, 1405 (1982); B. Zellner, in *Asteroids*, T. Gehrels, Ed. (Univ. of Arizona Press, Tucson, 1979), pp. 783–806; M. J. Gaffey and T. B. McCord, *Space Sci. Rev.* **21**, 555 (1978).
22. G. W. Wetherill, *Annu. Rev. Earth Planet. Sci.* **2**, 303 (1974).
23. C. R. Chapman, T. B. McCord, C. Pieters, *Astron. J.* **78**, 502 (1973); C. Pieters, M. J. Gaffey, C. R. Chapman, T. B. McCord, *Icarus* **28**, 105 (1976); M. A. Feierberg, H. P. Larson, C. R. Chapman, *Astrophys. J.* **257**, 361 (1982).
24. D. J. Tholen, thesis, University of Arizona, Tucson (1984).
25. M. J. Gaffey, *Icarus* **60**, 83 (1984).
26. V. F. Buchwald in *Handbook of Iron Meteorites* (Univ. of California Press, Berkeley, 1975), pp. 15–25; Z. Ceplecha and R. E. McCrosky, *J. Geophys. Res.* **81**, 6257 (1976).
27. P. R. Weissman and G. W. Wetherill, *Astron. J.* **79**, 404 (1974); R. S. Dunbar, thesis, Princeton University, Princeton (1980).

28. Supported by the Space Foundation of Houston, Texas, and NASA grants NSG 7323, NSG 7312, and NAGW 562. We thank G. W. Wetherill, L. A. Lebofsky, and an anonymous reviewer for their comments.

10 October 1984; accepted 8 March 1985

Phytoplankton Blooming Off the U.S. East Coast: A Satellite Description

Abstract. *A "bloom" of near-surface phytoplankton occurs in the Atlantic Slope region of the western Atlantic Ocean off the U.S. East Coast in the spring. Satellite time series of sea-surface temperature and phytoplankton pigment concentration, derived from measurements of the National Oceanic and Atmospheric Administration NOAA-7 Advanced Very-High-Resolution Radiometer and the National Aeronautics and Space Administration Nimbus-7 Coastal Zone Color Scanner, respectively, give information on the spatial extent and temporal development of such a bloom for a 28-day period in April through May 1982. The phytoplankton concentration of the slope area is comparable to that of the Atlantic Shelf. Total primary productivity of the slope during this period is equivalent to that of the shelf. The primary productivity within a warm-core ring and in the Gulf Stream system is less by a factor of 2.*

O. B. Brown
R. H. Evans
J. W. Brown
Division of Meteorology and Physical Oceanography, Rosenstiel School of Marine and Atmospheric Science, University of Miami, Miami, Florida 33149
H. R. Gordon
Department of Physics, University of Miami, Coral Gables, Florida 33124
R. C. Smith
Marine Bio-Optics Group, University of California at Santa Barbara, Santa Barbara 93106
K. S. Baker
Marine Bio-Optics Group, University of California at San Diego, La Jolla 92093

The "spring bloom" is a biological phenomenon that occurs during the temperate-zone transition from winter to spring in which phytoplankton are observed to grow rapidly. It is a dramatic example of the direct response of an oceanic biological process to changes in the physical environment. The classical explanation for the spring bloom was given by Riley (*1, 2*) and Sverdrup (*3*). During the winter, the breakdown of vertical stratification and the associated deep vertical mixing cause increased amounts of nutrients to be transferred into the euphotic zone. However, the same process cycles phytoplankton out of and into this zone (which is shallow in winter because of the reduced solar radiation incident on the sea surface). As a result, in winter the phytoplankton experience average light levels that are too low to allow net productivity in the water column, in spite of the elevated nutrient concentrations in the euphotic zone. The onset of the seasonal stratification, due to the warming of the surface waters in the spring, limits the vertical mixing to the upper tens of meters; this restricts the vertical movement of phytoplankton, for the most part, to the euphotic zone. Phytoplankton are then able to utilize this light- and nutrient-rich environment to reproduce in large numbers, thus blooming or flowering in a short period of time.

Typically, the concentration of chlorophyll *a* is used as an indicator of phytoplankton biomass because of the ease with which this quantity can be measured fluorometrically (*4*). In work with color imagery, however, the sum of the near-surface concentrations of chlorophyll *a* and pheopigments (henceforth referred to as the pigment concentration) is used as an index of phytoplankton biomass. At the pigment concentrations encountered, it should make no appreciable difference whether one uses the chlorophyll *a* concentration or the pigment concentration since the pheopigment concentration is typically only 10 percent or less of the chlorophyll *a* concentration (*5, 6*), which is well below the inherent error in our satellite-derived estimate of the pigment concentration (*7*).

Satellite imagery provides a synoptic view of the ocean surface over large areal extents and extended time periods, an accomplishment that was not possible with traditional oceanographic measurements. In the past, efforts have been made to acquire a time series of a particular region from repeated ship visits to single sites. For example, Menzel and Ryther (*8*) reported the results of one of the few complete long-term biological time series in the northwestern Sargasso Sea. They found that the chlorophyll *a* concentration in near-surface waters reached peak levels (1 mg m^{-3}) in early spring, dropped during the summer to 0.1 mg m^{-3}, rose slightly in the fall (0.5 mg m^{-3}), and then dropped again in late fall. However, they were not able to observe evolution of the spatial structure from their single station. Ryther and Yentsch (*9*) presented a biomass time series for the Atlantic Slope and the Atlantic Shelf, which indicated a bloom in the slope region (to 2 mg m^{-3}) during April. Their data (*9*) showed a major bloom (7 mg m^{-3}) on the shelf in February and March. Cox *et al.* (*10*) computed vertical profiles of chlorophyll on a monthly basis for the northern Sargasso Sea and the slope region. They found surface values in the slope waters of 0.45 mg m^{-3} in March, with maximum values of 2.9 mg m^{-3} in late April; these results underscore the difference in the timing and the magnitude of blooms in different regions off the U.S. East Coast. O'Reilly and Busch (*11*) presented data that emphasize the wide variety of blooms in subregions of the northwestern Atlantic Shelf waters. The slope region they examined was a narrow band near the shelf break, which reached a productivity maximum (1.5 g of carbon per square meter per day) in April and May whereas during the rest of the year it was half this amount.

The new satellite technology can provide a comprehensive overview of the surface temperature and pigments in several regions of the open ocean simultaneously. Data for four areas are presented here, including selected areas of the shelf, the slope, the Gulf Stream, and a